ARTICLE

Ionic Conduction and Fuel Cell Performance of $Ba_{0.98}Ce_{0.8}Tm_{0.2}O_{3-\alpha}$ Ceramic

Li-gan Qiu*, Mao-yuan Wang

School of Chemistry and Chemical Engineering, Yancheng Teachers University, Yancheng 224051, China

(Dated: Received on July 9, 2010; Accepted on October 29, 2010)

The perovskite-type oxide solid solution $Ba_{0.98}Ce_{0.8}Tm_{0.2}O_{3-\alpha}$ was prepared by high temperature solid-state reaction and its single phase character was confirmed by X-ray diffraction. The conduction property of the sample was investigated by alternating current impedance spectroscopy and gas concentration cell methods under different gases atmospheres in the temperature range of 500–900 °C. The performance of the hydrogen-air fuel cell using the sample as solid electrolyte was measured. In wet hydrogen, the sample is a pure protonic conductor with the protonic transport number of 1 in the range of 500–600 °C, a mixed conductor of proton and electron with the protonic transport number of 0.945–0.933 above 600 °C. In wet air, the sample is a mixed conductor of proton, oxide ion, and electronic hole. The protonic transport numbers are 0.010–0.021, and the oxide ionic transport numbers are 0.471–0.382. In hydrogen-air fuel cell, the sample is a mixed conductor of proton, oxide ion and electron, the ionic transport numbers are 0.942–0.885. The fuel cell using $Ba_{0.98}Ce_{0.8}Tm_{0.2}O_{3-\alpha}$ as solid electrolyte can work stably. At 900 °C, the maximum power output density is 110.2 mW/cm^2, which is higher than that of our previous cell using $Ba_xCe_{0.8}RE_{0.2}O_{3-\alpha}$ ($x\leq1$, RE=Y, Eu, Ho) as solid electrolyte.

Key words: $Ba_{0.98}Ce_{0.8}Tm_{0.2}O_{3-\alpha}$, Ionic conduction, Gas concentration cell, Alternating current impedance, Fuel cell

I. INTRODUCTION

Some trivalent rare earth ions doped perovskite-type ceramics based on $BaCeO_3$, $Ba_xCe_{1-y}RE_yO_{3-\alpha}$ exhibit good electrical properties at high temperature [1–3]. They have a vast range of perspective for applications as electrolytes in hydrogen-based energy, fuel cell, sensor, separation membrane, and other technologies [4, 5]. So they are attracting considerable attention. Nonstoichiomety ($x\neq1$) in these ceramics plays certain role in improving their performances. Ma *et al.* have studied the ionic conduction and nonstoichiometry in $Ba_xCe_{0.9}Y_{0.1}O_{3-\alpha}$ ($0.80\leq x\leq1.20$), discovering that $Ba_{0.95}Ce_{0.9}Y_{0.1}O_{3-\alpha}$ has not only the highest conductivities (0.12 S/cm in dry air, 0.11 S/cm in wet air, and 67 mS/cm in wet hydrogen, at 1000 °C), but also the highest chemical stability [6]. We have prepared $Ba_xCe_{0.8}RE_{0.2}O_{3-\alpha}$ ($x\leq1$, RE=Er, Y, Ho) and studied their defect structures, conduction properties, and hydrogen-air fuel cell performances, discovering the samples with $x<1$ have both higher conductivities and better fuel cell performances [7–9]. It may be correlated with their defect structures and oxidization-reduction [6–8]. For instance, in $Ba_{0.98}Ce_{0.8}RE_{0.2}O_{3-\alpha}$, RE^{3+} ions mainly exist in Ce^{4+}-sites, some RE^{3+} ions may transfer from Ce^{4+}-sites to Ba^{2+}-sites due to Ba^{2+} deficiency, but still leaving the Ba^{2+} vacancy and the corresponding O^{2-} vacancy. Its defect structure is as follows:

$$(\mathrm{Ba}_{\frac{0.98}{1-z}}\,\mathrm{RE}_{\frac{z}{1-z}}\,\square_{\frac{0.02-2z}{1-z}})(\mathrm{Ce}_{\frac{0.8}{1-z}}\,\mathrm{RE}_{\frac{0.2-z}{1-z}})\,\mathrm{O}_{3-\alpha}$$

where z and $\square$ represent the amount of RE^{3+} transferring from Ce^{4+}-sites to Ba^{2+}-sites and Ba^{2+} vacancy, respectively. Oxygen vacancy concentration α actually depends on z, that is, α in $Ba_{0.98}Ce_{0.8}RE_{0.2}O_{3-\alpha}$ is greater than that in $BaCe_{0.8}RE_{0.2}O_{3-\alpha}$, which helps to improve the ionic conductivities. Besides, partial Ce^{4+} on the surface of the ceramic may easily be reduced into Ce^{3+} under high temperature due to the lower alkaline caused by BaO deficiency, which produce electronic conduction to some extent, and thus increase the total conductivity and improve fuel cell performance. The higher chemical stability of $Ba_xCe_{1-y}RE_yO_{3-\alpha}$ ($x<1$) may be due to the lower alkaline caused by BaO deficiency [10]. Thus it is of great importance to prepare $Ba_xCe_{1-y}RE_yO_{3-\alpha}$ ($x<1$) perovskite-type oxides and study their electrical properties. However, there has been no detailed work done to study the preparation, electrical property, and application of $Ba_{0.98}Ce_{0.8}Tm_{0.2}O_{3-\alpha}$ solid electrolyte until now.

In this work, $Ba_{0.98}Ce_{0.8}Tm_{0.2}O_{3-\alpha}$ ceramic was pre-

*Author to whom correspondence should be addressed. E-mail: wmyqlg_64@hotmail.com

pared. The electrical conduction behavior of the sample was investigated under different gases atmospheres in the temperature range of 500–900 °C. The performance of hydrogen-air fuel cell using the ceramic as solid electrolyte was examined at 500–900 °C.

II. EXPERIMENTS

$Ba_{0.98}Ce_{0.8}Tm_{0.2}O_{3-\alpha}$ ceramic was prepared by the conventional solid-state reaction method [7]. The required amounts of $Ba(CH_3COO)_2$ (purity 99.0%), CeO_2 (99.95%), and Tm_2O_3 (99.95%) reagents were fully mixed in ethanol with an agate mortar and dried. The mixed powders were calcined at 1250 °C for 10 h in air. The obtained oxides were ground in ethanol using a planetary ball mill machine with an agate mill container and agate balls at 150 r/min for 5 h and dried by an infrared lamp, followed by sieving (100 mesh). The power was pressed into pellets by a hydrostatic pressing of 10 MPa, and sintered at 1550 °C for 20 h in air. The obtained ceramics were made into thin discs with the diameter of 14 mm and the thickness of 0.5 mm, which were applied to determine the electromotive forces (EMFs) of gas concentration cells and the current density-terminal voltage-power density (*I-V-P*) curves of the hydrogen-air fuel cell.

The sample phase was examined by powder X-ray diffraction analysis (XRD) using a nickel filtered Cu $K\alpha_I$ radiation (Rigaku D/MAX-III X-ray diffractometer). By alternating current (AC) impedance spectroscopy method over the frequency range of 12–10^5 Hz using a ZL5-Intelligent LCR measurer (made in Shanghai), the resistances of the sample were measured at 500–900 °C under wet hydrogen, wet air and hydrogen-air fuel cell atmospheres, respectively. The conductivity σ of the sample under these conditions was calculated from Eq.(1):

$$\sigma = \frac{L}{RS} \tag{1}$$

where L is thickness of the disc electrolytes, R is resistance, and S is electrode area.

For investigation of the ionic conduction and the performance of hydrogen-air fuel cell using the sample as electrolyte, the following gas concentration cell and hydrogen-air fuel cell were constructed:

Gas (I), Pt| $Ba_{0.98}Ce_{0.8}Tm_{0.2}O_{3-\alpha}$| Pt, gas (II)

H_2 (wet), Pt|$Ba_{0.98}Ce_{0.8}Tm_{0.2}O_{3-\alpha}$|Pt, air (wet)

where gas represents air, oxygen, hydrogen, or water vapor. Wet gas: saturated with H_2O at room temperature. Gas flow: 60 mL/min. The EMFs of gas concentration cell and *I-V-P* curves of hydrogen-air fuel cell were measured in the temperature range of 500–900 °C.

III. RESULTS AND DISCUSSION

A. Characterization

Figure 1 shows the powder XRD pattern of $Ba_{0.98}Ce_{0.8}Tm_{0.2}O_{3-\alpha}$. It is clear that the ceramic

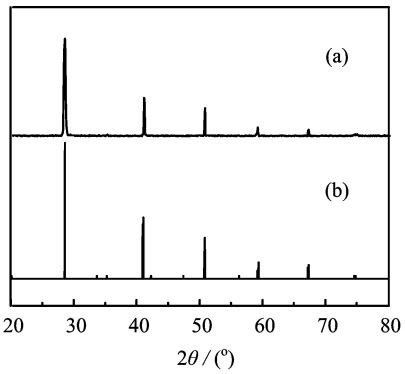

FIG. 1 Powder XRD pattern of (a) $Ba_{0.98}Ce_{0.8}Tm_{0.2}O_{3-\alpha}$ and (b) $BaCeO_3$ JCPDS (No.220074).

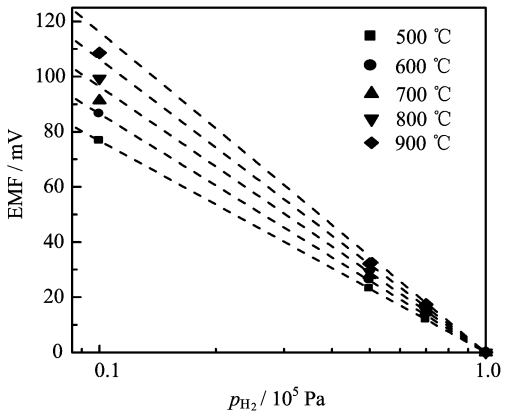

FIG. 2 EMF of the hydrogen concentration cell: H_2 (wet), Pt|$Ba_{0.98}Ce_{0.8}Tm_{0.2}O_{3-\alpha}$|Pt, H_2-Ar (wet).

shows a perovskite-type orthorhombic single phase, which corresponds to that of $BaCeO_3$ in JCPDS (No.220074). The color of the sintered ceramic is dark yellow-green and the relative density is higher than 92%. The experiment proved that the sintered ceramic could not be permeated by oxygen, air, or hydrogen.

B. Protonic conduction in wet hydrogen

Protonic conduction in $Ba_{0.98}Ce_{0.8}Tm_{0.2}O_{3-\alpha}$ ceramic in wet hydrogen was studied. The EMF values of the hydrogen concentration cell using the sample as solid electrolyte were measured at 500–900 °C, and the protonic transport number (t_{H^+}) was given by the ratio of the slope of each real line against that of each broken line at each temperature (Fig.2) [2, 11]. The total conductivity (σ_{H_2}) of the sample in wet hydrogen was measured, the protonic conductivity (σ_{H^+}) was calculated from the equation: $\sigma_{H^+}=\sigma_{H_2}t_{H^+}$, the electronic conductivity (σ_e) was calculated according to $\sigma_{H_2}= \sigma_{H^+}+\sigma_e$ [2, 11]. For comparison, σ_{H_2}, σ_{H^+}, and σ_e were all plotted in Fig.3.

DOI:10.1088/1674-0068/23/06/707-712

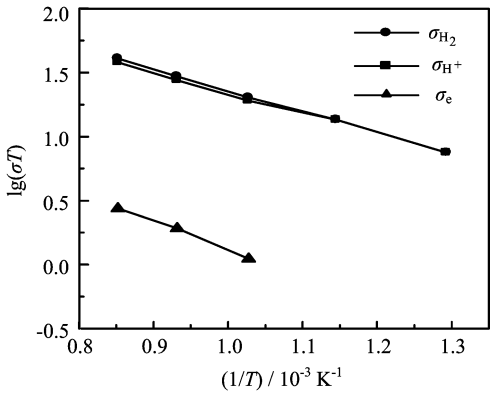

FIG. 3 Conductivities of $Ba_{0.98}Ce_{0.8}Tm_{0.2}O_{3-\alpha}$ in wet H_2 (p_{H_2O}=2.3 kPa).

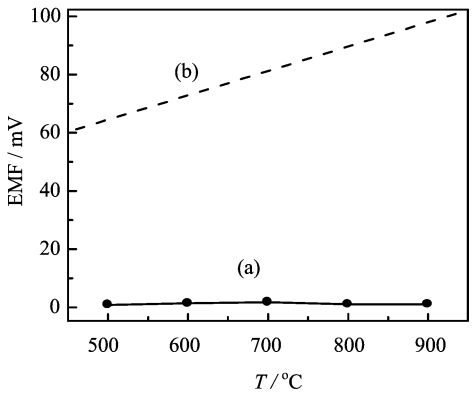

FIG. 4 EMF of the steam concentration cell: air (p'_{H_2O}), Pt|$Ba_{0.98}Ce_{0.8}Tm_{0.2}O_{3-\alpha}$|Pt, air ($p''_{H_2O}$). (a) Observed value and (b) theoretical value.

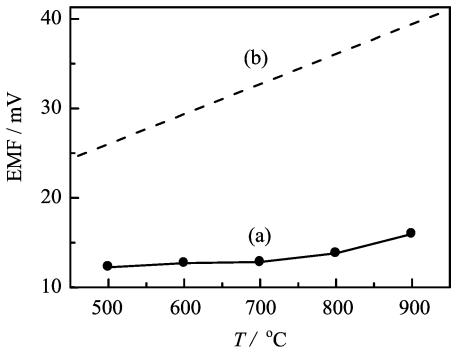

FIG. 5 EMF of the oxygen concentration cell: air (wet), Pt|$Ba_{0.98}Ce_{0.8}Tm_{0.2}O_{3-\alpha}$|Pt, O_2 (wet). (a) Observed value and (b) theoretical value.

Figure 2 is the EMF of the hydrogen concentration cell using $Ba_{0.98}Ce_{0.8}Tm_{0.2}O_{3-\alpha}$ as electrolyte at 500–900 °C. The broken line stands for the theoretical values at each temperature, obtained based on Nernst's equation [11]:

$$E_{\rm cal} = \frac{RT}{2F}\ln\frac{p_{H_2(I)}}{p_{H_2(II)}} \qquad (2)$$

where $p_{H_2(I)}$ and $p_{H_2(II)}$ are partial pressure of hydrogen in each compartment ($p_{H_2(I)}$=100 kPa, $p_{H_2(II)}$=10, 50, 70 kPa). R, T, and F have their usual meanings. The real line stands for the observed values ($E_{\rm obs}$). The water vapor pressure in both gases was kept constant (p_{H_2}=2.3 kPa).

It is evident from Fig.2 that the observed EMF values are in accordance with the theoretical ones at 500–600 °C and the protonic transport numbers are 1, suggesting that $Ba_{0.98}Ce_{0.8}Tm_{0.2}O_{3-\alpha}$ is a pure protonic conductor under such conditions. Above 600 °C, the observed EMF values are lower than the theoretical ones, and the protonic transport numbers are 0.945–0.933, indicating that $Ba_{0.98}Ce_{0.8}Tm_{0.2}O_{3-\alpha}$ is a mixed conductor of proton and electron, but protonic conduction is dominant.

Figure 3 shows the total, protonic and electronic conductivities of $Ba_{0.98}Ce_{0.8}Tm_{0.2}O_{3-\alpha}$ in wet hydrogen. It is seen from Fig.3 that lg(σT) increases with increasing temperature. At 500–600 °C, the total conductivity in wet hydrogen is regarded as the protonic conductivity. Above 600 °C, the protonic conductivity is slight lower than the total conductivity. At 900 °C, the total, protonic, and electronic conductivities of the sample in wet hydrogen are all maximum with 35, 32, and 3 mS/cm, respectively.

C. Ionic conduction in wet air

The ionic conduction in the ceramic sample under wet air was studied by the same method as that in wet hydrogen. At 500–900 °C, the EMF values of the steam concentration cell and the oxygen concentration cell using the sample as solid electrolyte were measured, and the results were shown in Fig.4 and Fig.5, respectively. The marks stand for the observed values ($E_{\rm obs}$), the broken lines stand for the theoretical values ($E_{\rm cal}$) at each temperature. The protonic and oxide ionic transport numbers (t_i) were thus obtained by the formula: t_i=$E_{\rm obs}/E_{\rm cal}$ [2, 11]. The total conductivity (σ_a) of the sample in wet air was measured, the protonic and oxide ionic conductivities (σ_i) were determined by the formula: σ_i=$\sigma_a t_i$, electronic hole conductivity σ_h can be calculated from the formula: σ_a=σ_{H^+}+$\sigma_{O^{2-}}$+σ_h [2, 11]. For comparison, σ_a, σ_{H^+}, $\sigma_{O^{2-}}$, and σ_h, were all plotted in Fig.6.

Figure 4 is the EMF of the steam concentration cell: air (p'_{H_2O}), Pt|$Ba_{0.98}Ce_{0.8}Tm_{0.2}O_{3-\alpha}$|Pt, air ($p''_{H_2O}$), where p'_{H_2O}>p''_{H_2O}, p'_{H_2O} and p''_{H_2O} were controlled by letting air pass through water at 30 and 0 °C, respectively. As shown in Fig.4, the EMF values are much smaller than the theoretical ones, the protonic transport numbers are 0.010–0.021, suggesting the sample shows very low protonic conduction in wet air at 500–900 °C.

DOI:10.1088/1674-0068/23/06/707-712

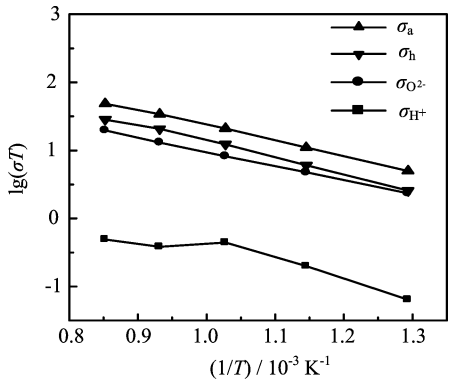

FIG. 6 Conductivities of $Ba_{0.98}Ce_{0.8}Tm_{0.2}O_{3-\alpha}$ in wet air.

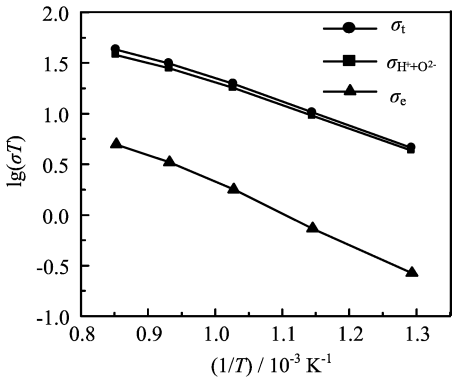

FIG. 7 Conductivities of $Ba_{0.98}Ce_{0.8}Tm_{0.2}O_{3-\alpha}$ in hydrogen-air fuel cell.

Figure 5 is the EMF of the oxygen concentration cell: air (wet), Pt|$Ba_{0.98}Ce_{0.8}Tm_{0.2}O_{3-\alpha}$|Pt, O_2 (wet). We can see from Fig.5 that the EMF values are smaller than the theoretical ones at each temperature, the oxide ionic transport numbers are 0.471–0.382, indicating that the sample exhibit low oxide ionic conduction in wet air at 500–900 °C.

Figure 6 shows the total, protonic, oxide ionic, and electronic hole conductivities of $Ba_{0.98}Ce_{0.8}Tm_{0.2}O_{3-\alpha}$ in wet air. It is clear that the conductivities of total, oxide ion, and electronic hole increase monotonically with temperature. The protonic conductivities increase monotonically from 500 °C to 700 °C, but decrease slightly above 700 °C, it may be ascribed the effect to competition between an increase in the mobility of protonic carriers due to thermal activation and a decrease in their concentration due to loss of water [2, 12]. However, the electronic hole conduction is always dominant in wet air under all experimental temperatures.

D. Ionic conduction in hydrogen-air fuel cell

For fuel cell: H_2 (wet), Pt|$Ba_{0.98}Ce_{0.8}Tm_{0.2}O_{3-\alpha}$|Pt, air (wet), the theoretical EMF values at different temperature were calculated based on Nernst's equation:

$$E_{\rm cal} = \frac{RT}{4F}\left\{\ln K - \ln\left[\frac{p_{\rm H_2O(A)}p_{\rm H_2O(B)}}{p^2_{\rm H_2(A)}p_{\rm O_2(B)}}\right]\right\} \qquad (3)$$

where K is the equilibrium constant for the cell reaction: $2H_2+O_2=H_2O(A)+H_2O(B)$. $p_{H_2(A)}$ and $p_{H_2O(A)}$ represent partial pressure of hydrogen and water vapor at the fuel electrode respectively, $p_{O_2(B)}$ and $p_{H_2O(B)}$ represent that of oxygen and water vapor at the air electrode respectively. The ionic transport numbers, $t_i=t_{H^+}+t_{O^{2-}}$, can be evaluated from the observed EMF values against the theoretical ones under certain temperature [13]. All the data are listed in Table I.

The total conductivity (σ_t) in hydrogen-air fuel cell includes the conductivities of ions (proton and oxide ion) and electron [14]. The ionic conductivity is determined by the formulas: $\sigma_i=\sigma_t t_i$, and σ_e can be calculated from the formula: $\sigma_e=\sigma_t-\sigma_i$. For comparison, σ_t, σ_i, and σ_e were all shown in Fig.7.

TABLE I Calculated EMFs ($E_{\rm cal}$), observed EMFs ($E_{\rm obs}$), ionic transport numbers (t_i), and electronic transport numbers (t_e) of the fuel cell.

T/°C	$E_{\rm cal}$/V	$E_{\rm obs}$/V	t_i	t_e
500	1.152	1.085	0.942	0.058
600	1.135	1.054	0.929	0.071
700	1.119	1.018	0.910	0.090
800	1.101	0.985	0.895	0.105
900	1.084	0.959	0.885	0.115

It is seen from Fig.7 that the conductivities of total, ion, and electron are increased with temperature. The electronic conductivity is very low, and the ionic conduction is always dominant in hydrogen-air fuel cell under all experimental temperatures.

E. Performance of hydrogen-air fuel cell

The typical discharge performance of the hydrogen-air fuel cell using $Ba_{0.98}Ce_{0.8}Tm_{0.2}O_{3-\alpha}$ as solid electrolyte is shown in Fig.8. A steady and stable current could be drawn from the cell, indicating that the ceramic diaphragm could serve as the solid electrolyte of a fuel cell. At 500–900 °C, the relation between terminal voltage and current output is linear, suggesting the resistance of the solid electrolyte is the major factor of the cell performance. The open circuit voltage decreases with temperature increasing. It means that the electronic transfer numbers increase and the ionic transfer numbers decrease with increasing temperature. However, the current density increases with increasing temperature, this may be explained by two aspects: (i) protonic conductivity changes slightly and oxide ionic conductivity improves markedly with increasing temperature, which re-

DOI:10.1088/1674-0068/23/06/707-712

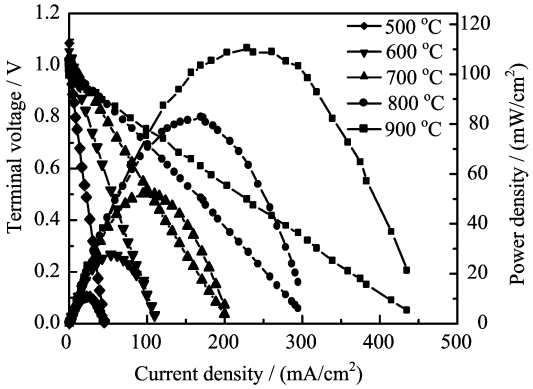

FIG. 8 *I-V-P* characteristic curves for the fuel cell: H_2 (wet), Pt|$Ba_{0.98}Ce_{0.8}Tm_{0.2}O_{3-\alpha}$|Pt, air (wet).

sults in the increase of general ionic conductivity; (ii) polarization effect at fuel electrode and air electrode decreases markedly with increasing temperature. Thus the discharge performance is improved [4]. The maximum power output density of the hydrogen-air fuel cell using $Ba_{0.98}Ce_{0.8}Tm_{0.2}O_{3-\alpha}$ as solid electrolyte is 110.2 mW/cm^2 at 900 °C, which is higher than that of our previous cell using $Ba_xCe_{0.8}RE_{0.2}O_{3-\alpha}$ ($x\leq1$, RE=Y, Eu, Ho) as electrolyte because of its higher conductivities in wet hydrogen and wet air [3, 4, 15].

IV. DEFECT CHEMISTRY

The defect chemistry in $Ba_{0.98}Ce_{0.8}Tm_{0.2}O_{3-\alpha}$ ceramic under different gas atmospheres was studied. Using Tm_2O_3 doped $BaCeO_3$, substitution of Tm^{3+} for Ce^{4+} may provide oxide ionic vacancies as a means of charge compensation:

$$Tm_2O_3 \rightarrow 2Tm'_{Ce} + 3O_o^{\times} + V_o^{\cdot\cdot} \tag{4}$$

where Tm'_{Ce}, $O_o^{\times}$, and $V_o^{\cdot\cdot}$ represent Tm^{3+} at the normal Ce^{4+}-sites, oxide ions, and oxide ionic vacancies at the normal O^{2-}-sites, respectively.

The oxide ionic vacancies may be in equilibrium with electronic holes:

$$V_o^{\cdot\cdot} + \frac{1}{2}O_2 \leftrightarrow O_o^{\times} + 2\ h^{\cdot} \tag{5}$$

where $h^{\cdot}$ represents electronic holes. The oxide ionic vacancies and electronic holes interact with different gaseous environment to produce a variety of point defects [1, 16].

In wet hydrogen, hydrogen reacts with electronic holes producing protons, which results in protonic conduction:

$$H_2 + 2\ h^{\cdot} \leftrightarrow 2H^+ \tag{6}$$

Above 600 °C, partial Ce^{4+} on the surface of $Ba_{0.98}Ce_{0.8}Tm_{0.2}O_{3-\alpha}$ ceramic can be reduced into Ce^{3+} in hydrogen due to the lower alkaline caused by BaO deficiency, which produces electronic conduction to some extent [4]. Its defect reaction may be shown as follows:

$$Ce_{Ce}^{\times} + e' \rightarrow Ce'_{Ce} \tag{7}$$

where $Ce_{Ce}^{\times}$ and Ce'_{Ce} represent Ce^{4+} and Ce^{3+} at the normal Ce^{4+}-sites, respectively. Thus the sample exhibits mixed conduction of proton and electron in wet hydrogen above 600 °C.

In wet air, the defect reactions may be expressed as reactions as shown in Eq.(4), Eq.(5) above and reaction Eq.(8) below:

$$V_o^{\cdot\cdot} + H_2O \leftrightarrow O_o^{\times} + 2H^+ \tag{8}$$

From the reaction shown in Eq.(4), we get to know that oxide ionic vacancies diffusion causes oxide ionic conduction. According to reactions shown in Eq.(5) and Eq.(8), oxide ionic vacancies react with oxygen and water vapor producing electronic holes and protons, resulting in electronic hole and protonic conduction, respectively. Thus the sample exhibits mixed conduction of oxide ion, proton and electronic hole in wet air.

In hydrogen-air fuel cell, the electrode reactions are expressed as reactions shown in Eq.(9) and Eq.(10) below, and the sample exhibits mixed conduction of oxide ion, proton, and electron [14].

Fuel electrode:

$$2H_2 + O^{2-} = 2H^+ + H_2O(A) + 4e^- \tag{9}$$

Air electrode:

$$O_2 + 2H^+ + 4e^- = H_2O(B) + O^{2-} \tag{10}$$

V. CONCLUSION

The sample of $Ba_{0.98}Ce_{0.8}Tm_{0.2}O_{3-\alpha}$ is a single phase of pervoskite-type orthorhombic structure. In wet hydrogen, $Ba_{0.98}Ce_{0.8}Tm_{0.2}O_{3-\alpha}$ is a pure protonic conductor at 500–600 °C, a mixed conductor of proton and electron above 600 °C due to its reduction. In wet air, the sample exhibits low protonic and oxide ionic conduction, the electronic hole conduction is always dominant at all experimental temperatures. In hydrogen-air fuel cell, the sample is a mixed conductor of proton, oxide ion and electron, and the ionic conduction is always dominant at 500–900 °C. The performances of the fuel cell using $Ba_{0.98}Ce_{0.8}Tm_{0.2}O_{3-\alpha}$ as solid electrolyte are better than that of $Ba_xCe_{0.8}RE_{0.2}O_{3-\alpha}$($x\leq1$, RE=Y, Eu, Ho), and at 900 °C, its maximum power output density is 110.2 mW/cm^2.

VI. ACKNOWLEDGMENTS

This work was supported by the National Natural Science Foundation of China (No.20771079), the

DOI:10.1088/1674-0068/23/06/707-712

Qing Lan Project, and the Natural Science Foundation of Education Department of Jiangsu Province (No.07KJB150126).

[1] H. Iwahara, H. Uchida, K. Kondo, and K. Ogaki, J. Electrochem. Soc. **135**, 529 (1988).
[2] N. Bonanos, Solid State Ionics **53-56**, 967 (1992).
[3] H. Iwahara, Solid State Ionics **86-88**, 9 (1996).
[4] H. Iwahara, Y. Asakura, K. Katahira, and M. Tanaka, Solid State Ionics **168**, 299 (2004).
[5] G. Marnellos and M. Stoukides, Science **282**, 98 (1998).
[6] G. L. Ma, T. Shimura, and H. Iwahara, Solid State Ionics **110**, 103 (1998).
[7] L. G. Qiu, G. L. Ma, and D. J. Wen, Solid State Ionics **166**, 69 (2004).
[8] M. Y. Wang and L. G. Qiu, Chin. J. Inorg. Chem. **25**, 339 (2009).
[9] G. L. Ma, L. G. Qiu, and R. Chen, Acta Chim. Sin. **60**, 2135 (2002).
[10] K. H. Ryu and S. M. Haile, Solid State Ionics **125**, 355 (1999).
[11] G. L. Ma, T. Shimura, and H. Iwahara, Solid State Ionics **120**, 51 (1999).
[12] L. G. Qiu, G. L. Ma, and D. J. Wen, Chin. J. Chem. **23**, 1641 (2005).
[13] G. L. Ma, R. A. Gu, H. Shi, R. Chen, L. G. Qiu, and D. X. Jia, Acta Chim. Sin. **59**, 2084 (2001).
[14] H. Iwahara, T. Shimura, and H. Matsumoto, Electrochemistry **68**, 154 (2000).
[15] L. G. Qiu, G. L. Ma, and X. H. Lu, Chin. J. Appl. Chem. **20**, 936 (2003).
[16] R. GlÖckner, M. S. Islam, and T. Norbg, Solid State Ionics **122**, 145 (1999).

DOI:10.1088/1674-0068/23/06/707-712